



Published in final edited form as:

*Bioconj Chem.* 2018 March 21; 29(3): 771–775. doi:10.1021/acs.bioconjchem.7b00761.

## Subcutaneous Nanodisc Vaccination with Neoantigens for Combination Cancer Immunotherapy

Rui Kuai<sup>#†‡</sup>, Xiaoqi Sun<sup>#†‡</sup>, Wenmin Yuan<sup>†‡</sup>, Yao Xu<sup>†‡</sup>, Anna Schwendeman<sup>†‡\*</sup>, and James J. Moon<sup>†‡§\*</sup>

<sup>†</sup>Department of Pharmaceutical Sciences, University of Michigan, Ann Arbor, Michigan 48109, United States

<sup>‡</sup>Biointerfaces Institute, University of Michigan, Ann Arbor, Michigan 48109, United States

<sup>§</sup>Department of Biomedical Engineering, University of Michigan, Ann Arbor, Michigan 48109, United States

<sup>#</sup> These authors contributed equally to this work.

### Abstract

While cancer immunotherapy provides new exciting treatment options for patients, there is an urgent need for new strategies that can synergize with immune checkpoint blockers and boost the patient response rates. We have developed a personalized vaccine nanodisc platform based on synthetic high-density lipoproteins for co-delivery of immunostimulatory agents and tumor antigens, including tumor-specific neoantigens. Here we examined the route of delivery, safety profiles, and therapeutic efficacy of nanodisc vaccination against established tumors. We report that nanodiscs administered via the subcutaneous (SC) or intramuscular (IM) routes were well tolerated in mice without any signs of toxicity. The SC route significantly enhanced nanoparticle delivery to draining lymph nodes, improved nanodisc uptake by antigen-presenting cells, and generated 7-fold higher frequency of neoantigen-specific T cells, compared with the IM route. Importantly, when mice bearing advanced B16F10 melanoma tumors were treated with nanodiscs plus anti-PD-1 and anti-CTLA-4 IgG therapy, the combination immunotherapy exerted potent antitumor efficacy, leading to eradication of established tumors in ~60% of animals. These results demonstrate nanodiscs customized with patient-specific tumor neopeptides as a safe and powerful vaccine platform for immunotherapy against advanced cancer.

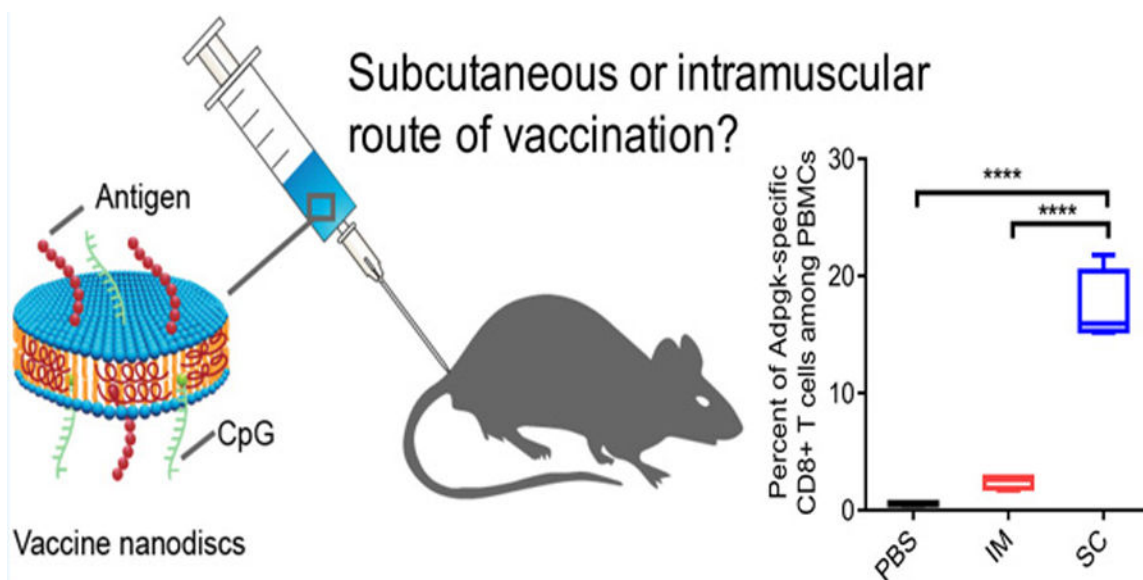
### Graphical abstract

**Corresponding Authors.** \* annaschw@umich.edu. \* moonjj@umich.edu.

The authors declare the following competing financial interest(s): A patent application for nanodisc vaccines has been filed, with J.J.M., A.S., and R.K. as inventors and with J.J.M. and A.S. as co-founders of EVOQ Therapeutics, LLC, that develops the nanodisc technology for vaccine applications.

Supporting Information

The Supporting Information is available free of charge on the ACS Publications website at DOI: 10.1021/acs.bioconjchem.7b00761. Materials and methods (PDF)



Cancer immunotherapy offers new hope for patients. As demonstrated in recent clinical trials, immune checkpoint blockers (ICBs), such as anti-PD-1 and anti-CTLA-4 IgG therapeutics, improve the overall patient survival rates for many cancer types, including advanced melanoma.<sup>1-4</sup> However, the response rates to ICBs generally remain below 30%.<sup>4</sup> Therefore, there is an urgent need to develop strategies that can boost the therapeutic potential of cancer immunotherapy.

We have previously reported a new nanovaccine technology based on synthetic high-density lipoprotein (sHDL) nanodiscs that can elicit potent antitumor T cell responses with robust therapeutic efficacy.<sup>5,6</sup> Briefly, we have shown that nanodiscs, composed of phospholipids and apolipoprotein A-1 mimetic peptides (22 amino acids in length), can co-deliver immunostimulatory agents and a variety of tumor antigens, including tumor-specific mutated neoantigens, to draining lymph nodes (dLNs) and generate strong antitumor cytotoxic T lymphocyte (CTL) responses.<sup>5</sup> Notably, nanodisc vaccination in combination with ICBs eliminated palpable B16F10 melanoma tumors in ~90% of animals.<sup>5</sup> While these results are promising, it remains to be seen whether these vaccine nanodiscs are effective against more advanced, established tumors. In addition, as the injection route is known to influence the efficacy of vaccines,<sup>7,8</sup> here we sought to examine the impact of administration route of nanodiscs. Namely, our previous studies were conducted using the SC route of vaccination, based on other reports documenting rapid lymphatic drainage of biomacromolecules and nanoparticles to dLNs after SC administration.<sup>9,10</sup> While the SC route of delivery has been widely employed for nanoparticle vaccines in preclinical development,<sup>11-15</sup> conventional vaccines used in the clinic are typically administered via the intramuscular (IM) route,<sup>16,17</sup> presumably due to the “depot” effect for prolonged vaccine delivery.<sup>18</sup> Therefore, with our long-term goal set on clinical translation of the nanovaccine technology, we have sought to address the following three questions in this current study: (1) to determine whether SC route of administration offers a superior site of nanodisc vaccination than the IM route; (2) to assess systemic and local safety profiles of nanodisc vaccination; (3) to thoroughly

evaluate the therapeutic efficacy of vaccine nanodiscs in combination with ICBs for treatment of advanced, established tumors.

Here, we first investigated the impact of administration routes on vaccine delivery to antigen-presenting cells (APCs) and induction of antigen (Ag)-specific T cell responses in mice. Specifically, we administered vaccine nanodiscs via the SC or IM route and studied their LN draining and uptake by different populations of APCs, including dendritic cells (DCs), B cells, and macrophages using IVIS and flow cytometry. We also analyzed serum biochemical markers and tissues from the injection sites and major organs after nanodisc vaccination for any signs of side effects. Briefly, our results showed that vaccine nanodiscs administered via the SC or IM routes were both well tolerated without any overt signs of systemic or local toxicity. Interestingly, compared with the IM route, the SC route of vaccination significantly improved nanodisc delivery to dLNs; promoted nanodisc uptake by DCs, B cells, and macrophages in dLNs; and elicited 7-fold higher frequency of Ag-specific T cell responses in mice. Lastly, when mice bearing advanced established B16F10 melanoma tumors (with the average tumor volume of  $\sim 80 \text{ mm}^3$  at the initiation of therapy) were treated with SC nanodisc vaccination plus ICBs, the combination immunotherapy induced robust CD8 $\alpha^+$  and CD4 $^+$  T cell responses against multiple tumor antigens, including neoantigens, and eradicated established B16F10 tumors in  $\sim 60\%$  of animals.

## RESULTS AND DISCUSSION

### Comparison of SC and IM Routes of Nanodisc Vaccination.

Vaccine nanodiscs containing the neoantigen Adpgk (sHDL-Adpgk/CpG) were prepared as we previously reported.<sup>5</sup> Briefly, the antigen peptide containing N-terminal cysteine was reacted with 1,2-dioleoyl-*sn*-glycero-3-phospho-ethanolamine (DOPE-PDP) to form lipid-peptide conjugate with  $>90\%$  of DOPE-PDP converted to the conjugate as determined by LC-MS. Lipid-peptide conjugate was then incubated with preformed nanodiscs for 30 min at room temperature to load them into the lipid bilayer of nanodiscs. The resulting sHDL nanodiscs were processed through desalting column to remove unincorporated reagents. We then incubated nanodiscs with CpG modified with cholesterol for 30 min at room temperature, with  $96.5 \pm 1.8\%$  of CpG incorporated into nanodiscs based on the gel permeation chromatography (GPC). sHDL-Adpgk/CpG had an average diameter of  $10.8 \pm 0.3 \text{ nm}$  and polydispersity index of  $0.22 \pm 0.02$  as measured by dynamic light scattering.

We then compared the effect of vaccination routes on induction of Ag-specific CD8 $\alpha^+$  T cell responses. We chose to focus on the SC and IM routes of vaccination because most vaccines in the clinic are administered via these two routes,<sup>16,17,19</sup> whereas cutaneous immunization via intradermal or transcutaneous routes requires skilled personnel or specialized injection apparatus and is often limited by small injection volume. We administered C57BL/6 mice with three weekly doses of sHDL-Adpgk/CpG via either the SC route at tail base or the IM route at thigh muscles bilaterally. One week after the third vaccination, peripheral blood mononuclear cells (PBMCs) were analyzed for the frequency of Adpgk neo-antigen-specific CD8 $\alpha^+$  T cells by tetramer staining and flow cytometry analyses. Mice immunized SC with nanodiscs elicited  $17.2 \pm 3.1\%$  Adpgk neoantigen-

specific CD8 $\alpha$ + T cells among PBMCs, representing a 7-fold increase compared with mice immunized IM with the equivalent dose of sHDL-Adpgk/CpG ( $p < 0.0001$ , Figure 1A,B).

We sought to investigate the impact of administration routes on nanodisc delivery to dLNs. We labeled nanodiscs with a lipophilic near-infrared fluorescent tracer, 1,1'-diiododecyl-3,3,3',3'-tetramethylindotricarbocyanine iodide (DiR), and administered them in C57BL/6 mice via either the SC or the IM route. After 24 h of injection, inguinal dLNs were harvested for ex vivo imaging by IVIS. The SC route of nanodisc administration significantly increased the DiR signal in inguinal dLNs, compared with the IM route (3.3-fold increase,  $p < 0.0001$ ; Figure 1C,D). We next prepared single cell suspensions from the dLNs and analyzed nanodisc uptake among various populations of APCs using flow cytometry. Consistent with the above results, the SC route of administration significantly increased cellular uptake of nanodiscs, as shown by improved mean fluorescence intensity (MFI) of DiR among CD11c+ DCs (1.3-fold,  $p < 0.05$ ), B220+ B cells (2.0-fold,  $p < 0.05$ ), and F4/80+ macrophages (1.5-fold), compared with the IM route of administration (Figure 1E–G). Taken together, these results indicated that compared with the IM route, the SC route of administration allows for more efficient delivery of nanodiscs to dLNs, resulting in improved nanodisc uptake by APCs in dLNs and induction of potent Ag-specific CD8 $\alpha$ + T cell responses in vivo.

### Safety of Nanodisc Vaccination.

To evaluate safety of nanodiscs, we injected C57BL/6 mice with three weekly doses of sHDL-Adpgk/CpG via the SC or the IM route. On day 7 after the third vaccination, we measured a series of serum biochemical markers, including sodium, potassium, calcium, chloride, triglyceride, cholesterol, albumin, total protein, aspartate aminotransferase (AST), alanine transaminase (ALT), and alkaline phosphatase (ALP) (Figure 2A). No significant changes were noted in animals that received PBS or nanodiscs via either the SC or the IM route. We also excised skin at the injection site, liver, and spleen on day 7 after the third vaccination and examined them after H&E staining. We did not observe any abnormal pathologies in the tissue sections (Figure 2B). Furthermore, in animals administered with nanodiscs, we did not observe any signs of weight loss (Supporting Information, Figure S1), any change in the body temperature (Supporting Information, Figure S2), acute release of IL-6, IL-12, IL-17, or TNF $\alpha$  in serum (Supporting Information, Figure S3), systemic toxicity, or autoimmunity. Overall, these results indicated that nanodisc vaccines were well tolerated without any overt systemic or local toxicity.

### Therapeutic Effects of Combination Immunotherapy.

Our results presented above have shown that the SC route of vaccine delivery significantly improved LN draining of nanodiscs, their uptake by APCs, and induction of Ag-specific CD8 $\alpha$ + T cell responses, compared with the IM route. On the basis of these results, we performed the subsequent therapeutic studies using the SC route of vaccination. In order to thoroughly evaluate the potential of our therapeutic strategy in a rigorous condition, we employed a highly aggressive and poorly immunogenic murine model of B16F10 melanoma. It is noted that B16F10 tumors are difficult to treat with conventional immunotherapies. For instance, multiple studies have shown that treatment of B16F10

tumor-bearing mice with anti-PD-1 and/or anti-CTLA-4 IgG therapies slowed tumor progression but failed to achieve regression or eradication of established B16F10 tumors.<sup>20–22</sup> In our current study, we inoculated C57BL/6 mice with  $1 \times 10^5$  B16F10 tumor cells in the SC flank on day 0 and initiated treatments on day 10 when advanced tumors (the average tumor volume of  $81 \pm 10 \text{ mm}^3$ ) were established (Figure 3A). On days 10, 17, 24, and 31, animals were treated with nanodiscs containing 2.3 nmol/dose of CpG and 10 nmol/dose of three multi-Ag peptides (MHC-I-restricted tumor-associated antigen tyrosinase-related protein 2, Trp2; and B16F10-specific neoantigens, including MHC-I-restricted M27 and MHC-II-restricted M30<sup>23,24</sup>). For the soluble control group, we administered the equivalent dose of multi-Ag peptides and CpG in the free form. For both treatment groups, we supplemented the vaccines with intra-peritoneal administration of anti-PD-1 and anti-CTLA-4 IgG antibodies on days 1 and 4 after each vaccination.

Compared with no treatment control group, mice treated with the soluble vaccine plus anti-PD-1/anti-CTLA-4 IgG therapy exhibited retardation of tumor growth (Figure 3B); however, 100% of animals eventually developed large tumors (Figure 3A,B) and succumbed to death with the median survival of 26 days (Figure 3C). In stark contrast, the combination immunotherapy with sHDL-multiAgs/CpG and anti-PD-1/anti-CTLA-4 IgG resulted in regression of established B16F10 tumors ( $p < 0.0001$ , Figure 3A,B), and 60% of animals remained tumor free until the end of the study at day 60 ( $p < 0.0001$ , compared with no treatment;  $p < 0.01$ , compared with soluble combo-immunotherapy; Figure 3C). The median duration of survival has not been reached at the end of the study for the sHDL-multiAgs/CpG plus anti-PD-1/anti-CTLA-4 IgG group. Furthermore, we examined specificity of antitumor T cell responses by performing ELISPOT analyses. Splenocytes harvested on day 24 from mice treated with sHDL-multiAgs/CpG and anti-PD-1/anti-CTLA-4 IgG responded robustly to MHC-I and MHC-II restricted Ag peptides (i.e., Trp2, M27, and M30), demonstrating significantly enhanced functional IFN- $\gamma$  T cell responses, compared with the soluble treatment group ( $p < 0.05$ , Figure 3D,E). Overall, these results have shown that vaccine nanodiscs elicit robust CD8 $\alpha$ <sup>+</sup> and CD4<sup>+</sup> T cell responses against multiple tumor antigens, including neoantigens and tumor-associated antigens, and that vaccine nanodiscs in combination with immune checkpoint blockers can exert remarkable antitumor efficacy against advanced B16F10 tumors.

## CONCLUSIONS

Nanodisc vaccination administered via the SC or IM routes were well tolerated without any significant systemic or local toxicities. However, the SC route of nanodisc vaccination generated significantly stronger T cell responses than the IM route, partially due to enhanced draining of nanodiscs to local draining lymph nodes and their increased uptake by antigen-presenting cells after SC administration. Moreover, SC nanodisc vaccination in combination with immune checkpoint blockers elicited robust CD8 $\alpha$ <sup>+</sup> and CD4<sup>+</sup> T cell responses against multiple tumor antigens and eliminated established B16F10 tumors in ~60% of animals. These results demonstrate strong efficacy of nanodiscs personalized with tumor neo-epitopes and offer a promising approach for combination immunotherapy against advanced cancers.

## Supplementary Material

Refer to Web version on PubMed Central for supplementary material.

## ACKNOWLEDGMENTS

This work was supported in part by NIH (Grant R01EB022563, J.J.M.; Grant R01CA210273, J.J.M.), MTRAC for Life Sciences Hub, UM Forbes Institute for Cancer Discovery Pilot Grant, and Emerald Foundation. J.J.M. is a Young Investigator supported by the Melanoma Research Alliance (Grant 348774), DoD/CDMRP Peer Reviewed Cancer Research Program (Grant W81XWH-16-1-0369), and NSF CAREER Award (Grant 1553831). R.K. is supported by the Broomfield International Student Fellowship and the AHA Predoctoral Fellowship (Grant 15PRE25090050). W.Y. is supported by AHA Postdoctoral Fellowship (Grant 16POST27760002). We acknowledge Lukasz Ochyl for critical review of the manuscript, and the NIH Tetramer Core Facility (Contract HHSN272201300006C) for provision of MHC-I tetramers. Opinions, interpretations, conclusions, and recommendations are those of the authors and are not necessarily endorsed by the Department of Defense.

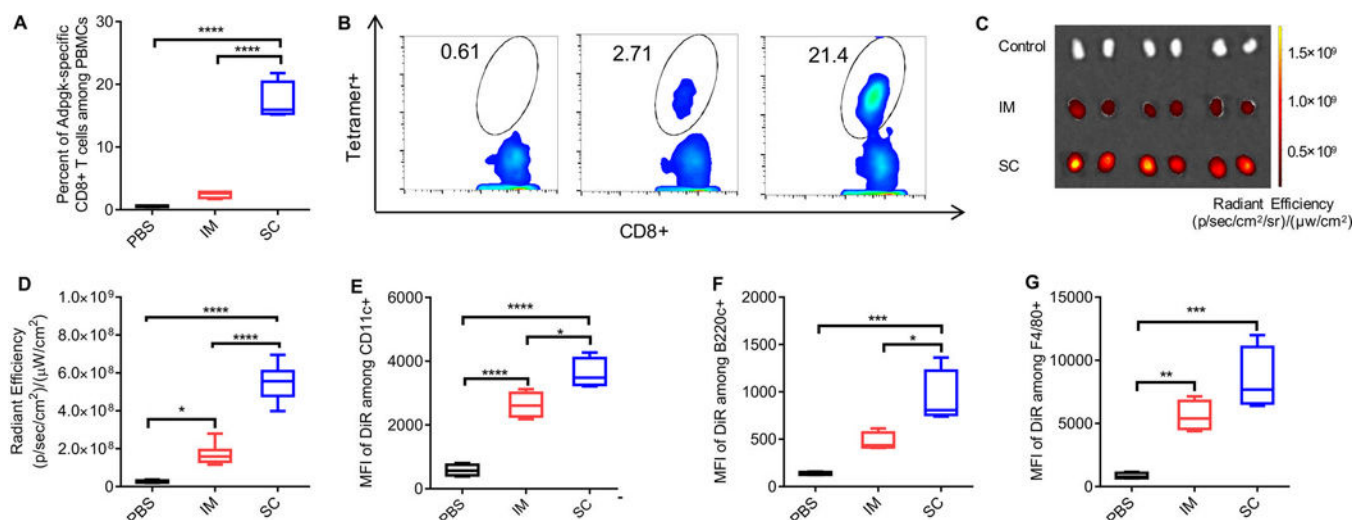
## REFERENCES

- (1). Pardoll DM (2012) The blockade of immune checkpoints in cancer immunotherapy. *Nat. Rev. Cancer* 12, 252–264.22437870
- (2). Hodi FS , O'Day SJ , McDermott DF , Weber RW , Sosman JA , Haanen JB , Gonzalez R , Robert C , Schadendorf D , Hassel JC , et al. (2010) Improved survival with ipilimumab in patients with metastatic melanoma. *N. Engl. J. Med* 363, 711–723.20525992
- (3). Topalian SL , Hodi FS , Brahmer JR , Gettinger SN , Smith DC , McDermott DF , Powderly JD , Carvajal RD , Sosman JA , Atkins MB , et al. (2012) Safety, activity, and immune correlates of anti-PD-1 antibody in cancer. *N. Engl. J. Med* 366, 2443–2454.22658127
- (4). Robert C , Schachter J , Long GV , Arance A , Grob JJ , Mortier L , Daud A , Carlino MS , McNeil C , Lotem M , et al. (2015) Pembrolizumab versus ipilimumab in advanced melanoma. *N. Engl. J. Med* 372, 2521–2532.25891173
- (5). Kuai R , Ochyl LJ , Bahjat KS , Schwendeman A , and Moon JJ (2017) Designer vaccine nanodiscs for personalized cancer immunotherapy. *Nat. Mater* 16, 489–496.28024156
- (6). Kuai R , Li D , Chen YE , Moon JJ , and Schwendeman A (2016) High-Density Lipoproteins: Nature's Multifunctional Nano-particles. *ACS Nano* 10, 3015–3041.26889958
- (7). Mohanan D , Slutter B , Henriksen-Lacey M , Jiskoot W , Bouwstra JA , Perrie Y , Kundig TM , Gander B , and Johansen P (2010) Administration routes affect the quality of immune responses: A cross-sectional evaluation of particulate antigen-delivery systems. *J. Controlled Release* 147, 342–349.
- (8). Zhang P , Andorko JI , and Jewell CM (2017) Impact of dose, route, and composition on the immunogenicity of immune polyelectrolyte multilayers delivered on gold templates. *Biotechnol. Bioeng* 114, 423–431.27567213
- (9). Reddy ST , van der Vlies AJ , Simeoni E , Angeli V , Randolph GJ , O'Neil CP , Lee LK , Swartz MA , and Hubbell JA (2007) Exploiting lymphatic transport and complement activation in nanoparticle vaccines. *Nat. Biotechnol* 25, 1159–1164.17873867
- (10). Irvine DJ , Hanson MC , Rakhra K , and Tokatlian T (2015) Synthetic Nanoparticles for Vaccines and Immunotherapy. *Chem. Rev* 115, 11109–11146.26154342
- (11). Oussoren C , Zuidema J , Crommelin DJ , and Storm G (1997) Lymphatic uptake and biodistribution of liposomes after subcutaneous injection. II. Influence of liposomal size, lipid composition and lipid dose. *Biochim. Biophys. Acta, Biomembr* 1328, 261–272.
- (12). Sahdev P , Ochyl LJ , and Moon JJ (2014) Biomaterials for nanoparticle vaccine delivery systems. *Pharm. Res* 31, 2563–2582.24848341
- (13). Fan YC , and Moon JJ (2015) Nanoparticle Drug Delivery Systems Designed to Improve Cancer Vaccines and Immunotherapy. *Vaccines (Basel, Switz.)* 3, 662–685.
- (14). Moynihan KD , Opel CF , Szeto GL , Tzeng A , Zhu EF , Engreitz JM , Williams RT , Rakhra K , Zhang MH , Rothschilds AM , et al. (2016) Eradication of large established tumors in mice by



combination immunotherapy that engages innate and adaptive immune responses. *Nat. Med* 4, 1402–1410.

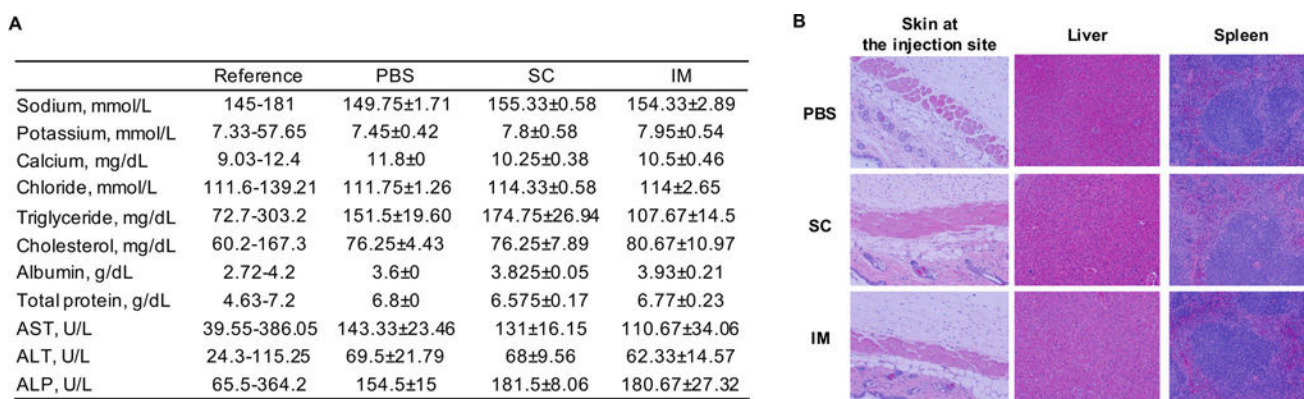
- (15). Zhang W , An M , Xi J , and Liu H (2017) Targeting CpG Adjuvant to Lymph Node via Dextran Conjugate Enhances Antitumor Immunotherapy. *Bioconjugate Chem* 28, 1993–2000.
- (16). Dennehy PH , Reisinger KS , Blatter MM , and Veloudis BA (1991) Immunogenicity of subcutaneous versus intramuscular Oka/ Merck varicella vaccination in healthy children. *Pediatrics* 88, 604–607.1881743
- (17). Diez-Domingo J , Weinke T , Garcia de Lomas J , Meyer CU , Bertrand I , Eymin C , Thomas S , and Sadorge C (2015) Comparison of intramuscular and subcutaneous administration of a herpes zoster live-attenuated vaccine in adults aged  $\geq 50$  years: a randomised non-inferiority clinical trial. *Vaccine* 33, 789–795.25555381
- (18). Chattopadhyay S , Chen JY , Chen HW , and Hu CJ (2017) Nanoparticle Vaccines Adopting Virus-like Features for Enhanced Immune Potentiation. *Nanotheranostics* 1, 244–260.29071191
- (19). Mark A , Carlsson RM , and Granstrom M (1999) Subcutaneous versus intramuscular injection for booster DT vaccination of adolescents. *Vaccine* 17, 2067–2072.10217608
- (20). Curran MA , Montalvo W , Yagita H , and Allison JP (2010) PD-1 and CTLA-4 combination blockade expands infiltrating T cells and reduces regulatory T and myeloid cells within B16 melanoma tumors. *Proc. Natl. Acad. Sci. U. S. A* 107, 4275–4280.20160101
- (21). Twyman-Saint Victor C , Rech AJ , Maity A , Rengan R , Pauken KE , Stelekati E , Benci JL , Xu B , Dada H , Odorizzi PM , et al. (2015) Radiation and dual checkpoint blockade activate non-redundant immune mechanisms in cancer. *Nature* 520, 373–377.25754329
- (22). De Henau O , Rausch M , Winkler D , Campesato LF , Liu CL , Hirschhorn-Cymerman D , Budhu S , Ghosh A , Pink M , Tchaicha J , et al. (2016) Overcoming resistance to checkpoint blockade therapy by targeting PI3K gamma in myeloid cells. *Nature* 539, 443–447.27828943
- (23). Castle JC , Kreiter S , Diekmann J , Lower M , Van de Roemer N , de Graaf J , Selmi A , Diken M , Boegel S , Paret C , et al. (2012) Exploiting the Mutanome for Tumor Vaccination. *Cancer Res* 72, 1081–1091.22237626
- (24). Kreiter S , Vormehr M , van de Roemer N , Diken M , Lower M , Diekmann J , Boegel S , Schrors B , Vascotto F , Castle JC , et al. (2015) Mutant MHC class II epitopes drive therapeutic immune responses to cancer. *Nature* 520, 692–696.25901682



**Figure 1.**

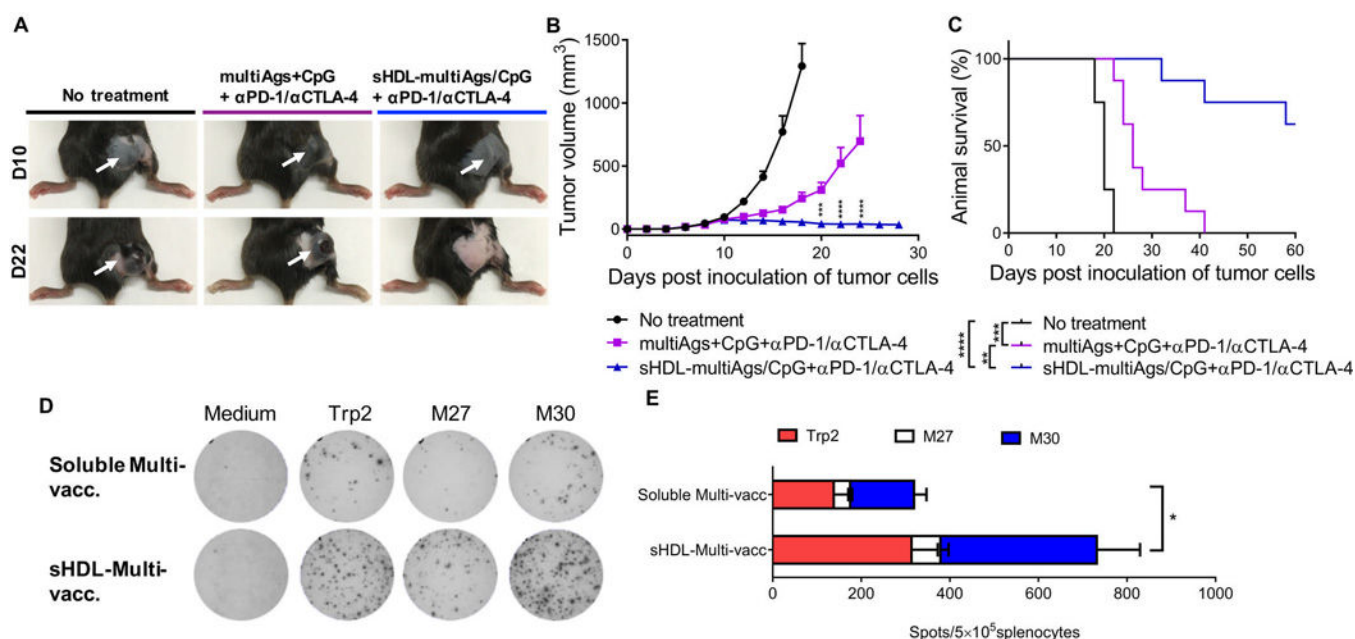
Effect of administration routes of vaccine nanodiscs on antigen-specific CD8 $\alpha$ <sup>+</sup> T cell responses. (A, B) C57BL/6 mice were vaccinated with three doses of nanodiscs containing 15.5 nmol/dose of neoantigen Adpgk peptide and 2.3 nmol/dose of CpG through the IM or SC route in a 1-week interval. On day 7 after the last vaccination, antigen-specific CD8 $\alpha$ <sup>+</sup> T cell responses were measured by the tetramer staining assay. Shown are (A) the percentages of Adpgk-specific CD8 $\alpha$ <sup>+</sup> T cells and (B) representative flow cytometry scatter plots. (C, D) C57BL/6 mice were injected with nanodiscs containing 1  $\mu$ g/dose of DiR via the SC or IM route. At 24 h after injection, mice were euthanized and inguinal lymph nodes were harvested for IVIS imaging. (E–G) C57BL/6 mice were injected with nanodiscs containing 1  $\mu$ g/dose of DiR via the SC or IM route. At 24 h after injection, uptake of nanodiscs by different antigen-presenting cells in draining inguinal lymph nodes was measured by flow cytometry. Shown are the uptake of nanodiscs by dendritic cells (CD11c<sup>+</sup>), B cells (B220<sup>+</sup>), and macrophages (F4/80<sup>+</sup>). Data are represented as box plots (whiskers 5–95 percentile,  $n = 3$ –4): (\*)  $P < 0.05$ , (\*\*)  $P < 0.01$ , (\*\*\*)  $P < 0.001$ , and (\*\*\*\*)  $P < 0.0001$  analyzed by one-way ANOVA with Bonferroni multiple comparisons post-test.





**Figure 2.**

Safety of nanodisc vaccination. (A, B) C57BL/6 mice were vaccinated with three doses of nanodiscs containing 15.5 nmol/dose of neoantigen Adpgk peptide and 2.3 nmol/dose of CpG via the SC or IM route in a 1-week interval. On day 7 after the last vaccination, mice were euthanized for (A) analyses of serum biochemical markers and (B) H&E staining for histological analyses of the injection site and major organs. Data are represented as mean  $\pm$  SD ( $n = 4$ ).

**Figure 3.**

Therapeutic effect of vaccine nanodiscs in combination with immune checkpoint blockers. (A–C) C57BL/6 mice were inoculated subcutaneously with  $1 \times 10^5$  B16F10 tumor cells on day 0. On days 10, 17, 24, and 31, tumor-bearing mice were treated with indicated formulations containing 10 nmol/dose of each antigen peptide (Trp2, M27, and M30) and 2.3 nmol/dose of CpG. Anti-PD-1 (100  $\mu$ g/dose) and anti-CTLA-4 (100  $\mu$ g/dose) IgG were injected intraperitoneally on days 1 and 4 after each vaccination. Shown are (A) representative pictures of tumor-bearing mice on day 10 (at the start of treatment) and day 22 with arrows pointing to tumors, (B) the average tumor growth, and (C) animal survival. Data represent the mean  $\pm$  SEM ( $n = 8$ ). (D, E) On day 24, tumor antigen-specific T cell responses were assessed by IFN- $\gamma$  ELISPOT analysis. Shown are (D) representative pictures of ELISPOT wells and (E) the number of IFN- $\gamma$  spots specific to the indicated tumor antigens. Data represent the mean  $\pm$  SEM ( $n = 5$ –8): (\*)  $P < 0.05$ , (\*\*)  $P < 0.01$ , (\*\*\*)  $P < 0.001$ , and (\*\*\*\*)  $P < 0.0001$  analyzed by two-way ANOVA (B), one-way ANOVA (E) with Bonferroni multiple comparisons post-test, or log rank (Mantel–Cox) test (C).